JVI Journals.ASM.org

Immune Activation and Regulation in Simian Immunodeficiency Virus-*Plasmodium fragile*-Coinfected Rhesus Macaques

Kristin A. Trott,[a] Amy Richardson,[b] Michael A. Hudgens,[b] Kristina Abel[c]

California National Primate Research Center, University of California at Davis, Davis, California, USA[a]; Gillings School of Public Health, University of North Carolina at Chapel Hill, Chapel Hill, North Carolina, USA[b]; Department of Microbiology and Immunology, University of North Carolina at Chapel Hill, Chapel Hill, North Carolina, USA[c]

Human immunodeficiency virus (HIV) is characterized by immune activation, while chronic malaria is associated with elevated interleukin-10 (IL-10) levels. How these apparently antagonizing forces interact in the coinfected host is poorly understood. Using a rhesus macaque model of simian immunodeficiency virus (SIV)-*Plasmodium fragile* coinfection, we evaluated how innate immune effector cells affect the balance between immune activation and regulation. *In vitro* Toll-like receptor (TLR) responses of peripheral blood myeloid dendritic cells (mDC) and monocytes were temporarily associated with acute parasitemic episodes and elevated plasma IL-10 levels. Prolonged infection resulted in a decline of mDC function. Monocytes maintained TLR responsiveness but, in addition to IL-12 and tumor necrosis factor alpha, also produced IL-10. Consistent with the role of spleen in the clearance of parasite-infected red blood cells, coinfected animals also had increased splenic IL-10 mRNA levels. The main cellular source of IL-10 in the spleens of coinfected animals, however, was not splenic macrophages but T cells, suggesting an impairment of adaptive immunity. In contrast to those in spleen, IL-10-positive cells in axillary lymph nodes of coinfected animals were predominantly mDC, reminiscent of the immunosuppressive phenotype of peripheral blood mDC. Concurrent with IL-10 induction, however, SIV infection promoted elevated systemic IL-12 levels. The continuously increasing ratio of plasma IL-12 to IL-10 suggested that the overall host response in SIV-*P. fragile*-coinfected animals was shifted toward immune activation versus immune regulation. Therefore, SIV-*P. fragile* coinfection might be characterized by earlier manifestation of immune dysfunction and exhaustion than that of single-pathogen infections. This could translate into increased morbidity in HIV-malaria-coinfected individuals.

Coinfection of human immunodeficiency virus (HIV) with malaria has been associated with more severe disease and also with higher transmission risk (1–8). Increased morbidity is indicative of reduced host immunity to HIV, malaria, or both. If we can define specific immune mechanisms that are altered in coinfection compared to infection with either pathogen alone, we might be able to develop more effective intervention methods. Toward this goal, we developed a rhesus macaque model of simian immunodeficiency virus (SIV)-*Plasmodium fragile* coinfection to study HIV-*P. falciparum* infection in humans (9). Using this model, we were able to demonstrate that SIV-*P. fragile*-coinfected rhesus macaques experienced increased viremia and gametocytemia during primary parasitemia (9), a finding consistent with human data showing the potential for an increased transmission risk of both HIV and malaria in coinfected individuals (3–5, 10, 11). Reasoning that primary parasitemia represents a very early time point in coinfection, we hypothesized that altered innate responses must have contributed to the temporarily reduced control of virus and parasite replication. The current study used archived specimens from the animals of our previously described study (9) and focused on the functional analysis of myeloid dendritic cells and monocytes/macrophages as key players in pathogen recognition, antigen presentation, and induction of adaptive immune responses, as well as in the balance between immune activation and regulation.

Monocytes (Mo), macrophages (Mph), and myeloid dendritic cells (mDC) express pathogen recognition receptors, such as Toll-like receptors (TLR), that recognize conserved microbial patterns and shape the ensuing innate and adaptive immune responses. During acute malaria, expression of TLR and responses to TLR stimulation are heightened and dominated by a proinflammatory profile (12). These responses are dampened concurrently with the clearance of parasite-infected erythrocytes to avoid exorbitant inflammation that could result in excess pathology and erythrocyte depletion (13–16).

Interleukin-10 (IL-10) plays an important role in the immune regulation of malaria infection (12, 17–19). In fact, IL-10 deficiency results in extreme pathology (20). Malaria parasites and free hemozoin (Hz), a by-product of heme degradation by malaria parasites, can induce IL-10. At the same time, persistently elevated levels of IL-10 due to sustained levels of Hz in chronic malaria have been shown to inhibit TLR-mediated mDC function and interfere with malarial immunity (21–23). Similarly, HIV infection negatively affects TLR responses of mDC and Mo/Mph. In acute HIV infection, mDC cytokine production is increased following TLR stimulation due to upregulation of receptors (24–26). At the same time, monocytes become hyperactivated and show reduced maturation into dendritic cells (24, 25, 27, 28). The persistent immune activation in HIV infection will eventually lead to immune exhaustion (29–32). Similar to its role in malaria infection, the immunoregulatory cytokine IL-10 plays an important role in the balance between immune activation and regulation. Although IL-10 will likely limit immunopathogenesis by inflammatory mediators, in many chronic viral infections, IL-10-medi-

Received 29 March 2013 **Accepted** 13 June 2013
Published ahead of print 19 June 2013
Address correspondence to Kristina Abel, Abelk@med.unc.edu.

doi:10.1128/JVI.00861-13

ated suppression of adaptive immunity concurrently allows for chronic antigenic stimulation, subsequent exhaustion, and eventual failure of immunity (33, 34).

Therefore, we hypothesized that the exacerbated morbidity in HIV-malaria coinfection was due to an imbalanced immune response shifted toward excess immune activation resulting in failure of innate, and thereby adaptive, responses. Our data show that innate immune cells, specifically Mo/Mph and mDC, displayed altered *in vitro* function during SIV-*P. fragile* coinfections. Periods of altered *in vitro* TLR responses were temporarily associated with *in vivo* elevations of plasma IL-10 induced by the malaria parasite. Impaired innate responses were also reflected in IL-10-producing mDC in spleens of SIV-*P. fragile*-coinfected animals. Concurrently, however, SIV-induced immune activation resulted in a net immune response that was skewed toward inflammation, thereby promoting increased immune T cell exhaustion and dysfunction.

MATERIALS AND METHODS

Animals and infections. Tissues, plasma, and cell suspensions were collected from adult male rhesus macaques infected with SIV or *Plasmodium fragile* or coinfected with both, as previously described (9). Animals were obtained from the California National Primate Research Center (CNPRC) and housed in accordance with the regulations of the American Association for Assessment and Accreditation of Laboratory Animal Care (AAALAC) at the CNPRC. All animal procedures were reviewed and approved by the UC Davis Institutional Animal Care and Use Committee (IACUC) prior to study initiation. Briefly, SIV infections were performed via intravenous (i.v.) inoculation with 10^3 50% tissue culture infectious doses ($TCID_{50}$) of SIVmac239. Malaria infections were established via i.v. inoculation with 1×10^6 to 2×10^6 *P. fragile*-infected rhesus macaque erythrocytes. Malaria-infected animals were subsequently treated with subcurative doses (150 mg) of quinine sulfate (Qualaquin; URL Pharma, Inc., Philadelphia, PA) via orogastric intubation for 2 (*P. fragile*-infected animals) or 4 (SIV-*P. fragile*-coinfected animals) consecutive days when parasitemia rose above 0.5%. Coinfected animals were inoculated with SIV 28 days prior to *P. fragile* infection. Groups consisted of the following animals: SIV (32975 and 33677), *P. fragile* (33308, 33959, and 36346), and SIV-*P. fragile* (35914, 37007, and 37009) (9).

During the acute stage of malaria infection, blood was collected every other day to monitor hematocrit and parasitemia. Thereafter, blood samples were collected weekly for parasitologic, virologic, and immunologic analyses. At necropsy, lymphoid tissues, liver, and brain were collected for histological analysis.

For consistency in comparing various parameters between groups, data are reported as days postinfection with SIV (DPI-SIV) regardless of actual infection with SIV. Therefore, an animal only infected with *P. fragile* would be infected with *P. fragile* at 28 DPI-SIV or 0 days postinfection with *P. fragile* (DPI-Pf 0), so that the animal can be compared to a SIV-*P. fragile*-coinfected animal at the same time periods in the course of malaria (i.e., acute malaria occurring at DPI-SIV 42 or DPI-Pf 14).

Plasma cytokines. Plasma IL-10 and IL-12 levels were measured via enzyme-linked immunosorbent assay (ELISA) (UCytech, Netherlands), and plasma tumor necrosis factor alpha (TNF-α), gamma interferon (IFN-γ), IL-2, and IL-6 were measured by a cytokine bead array (BD, San Jose, CA), both per the manufacturers' protocols.

***In vitro* TLR stimulation.** To test mDC and Mo responsiveness to TLR2, TLR4, and TLR7/8, peripheral blood mononuclear cells (PBMC) were stimulated with media, 1 μg/ml lipomannan (LPM), 1 μg/ml lipopolysaccharide (LPS), or 5 μg/ml R848, respectively (all from Invivogen, San Diego, CA). Cultures were stimulated for 5 h at 37°C and 5% CO_2. After 1 h of incubation, 10 μg/ml brefeldin A (eBiosciences, San Diego, CA) was added to cultures. At the end of the culture period, cells were stained according to the BD protocol using the following antibodies: CD3 (clone SP34-2; BD, San Jose, CA), CD14 (clone M5E2; BD), CD20 (clone 2H7; BD), HLA-DR (clone L243; BD), CD11c (clone S-HCL-3; BD), TNF-α (clone MAB11; eBioscience), IL-12 (clone C8.6; eBiosciences), and IL-10 (clone JES3-9D7; Miltenyi Biotec, Auburn, CA). Myeloid DC were defined as lineage marker negative ($CD3^-$, $CD14^-$, $CD20^-$), $HLA\text{-}DR^+$, and $CD11c^+$. Monocytes were defined as $CD3^-$, $CD20^-$, and $CD14^+$. Data were reported as frequency of mDCs or Mo positive for IL-12, TNF-α, or IL-10, subtracting the mediaum control from stimulated samples. All flow-cytometric data were acquired on a FACSAria (BD, San Jose, CA) using FACS DIVA software and analyzed with FlowJo (TreeStar, Inc., Ashland, OR).

TLR PCR array. RNA was isolated from whole-spleen samples preserved in RNAlater using the Qiagen RNeasy microarray tissue RNA isolation kit. Subsequently, cDNA was prepared with the Qiagen RT^2 first-strand cDNA kit and amplified using the rhesus macaque TLR PCR array (SA Biosciences/Qiagen). All protocols were performed according to the manufacturer's instructions. Data were analyzed using the online RT^2 Profiler PCR array data analysis software, version 3.5.

Immunofluorescence. Tissues were collected at the time of necropsy, fixed in 10% formalin for 24 h, and then transferred to 70% ethanol until paraffin embedding. Sections for hematoxylin and eosin staining and immunofluorescence were cut at 5 μm. Tissues were rehydrated in a gradient of xylene (3 washes at 5 min each) and ethanol (100, 90, 85, and 50%; 3 min each) incubations and washed 2 times in distilled water (3 min each). Antigen retrieval was performed with target retrieval solution, pH 7 (Dako, Carpinteria, CA), for all staining protocols except for IL-10/DC-SIGN/CD205-stained sections, which used antigen retrieval AR-10 (BioGenex, Fremont, CA). Tissues were blocked with Background Eraser blocking reagent (Biocare Medical, Concord, CA) and 5% bovine serum albumin (BSA) and stained with mouse anti-human CD68 (clone KP1; mIgG1; 1×; Invitrogen, Grand Island, NY), rat anti-human CD3 (polyclonal rat; 1:10; UC Davis School of Veterinary Medicine), mouse anti-human CD20 (mIgG2a; 1:200; Dako), mouse IgG1 anti-human DEC205 (Leica Biosystems, Buffalo Grove, IL), mouse IgG_{2b} anti-human DC-SIGN (R&D Systems, Inc., Minneapolis, MN), rabbit anti-human cleaved caspase 3 (polyclonal rabbit; 1:200; Cell Signaling, Danvers, MA), and/or rabbit anti-human IL-10 (polyclonal rabbit; 1:200; AbCam, Cambridge, MA) supplemented with 2% rhesus macaque serum. Antibodies then were labeled with goat anti-mouse IgG1 Alexa Fluor 488, goat anti-mouse IgG1, goat anti-mouse IgG2a Alexa Fluor 488, goat anti-rat IgG Alexa Fluor 568, and/or goat anti-rabbit IgG Alexa Fluor 568 (all from Invitrogen, Grand Island, NY). Slides were coverslipped with Prolong gold with 4′,6-diamidino-2-phenylindole (DAPI) (Invitrogen). Proper isotype controls were used to control for nonspecific staining.

Caspase 3- and CD20/IL-10-stained images were acquired on an Olympus BX61 with a Photometrics CoolSnap camera using Slidebook automated capture software (version 4.1.0.4; Intelligent Imaging Innovations Inc.). Between 50 and 100 images (400× magnification) were captured per tissue section, covering approximately 7.5% of lymph node and 2.5% of spleen tissue. For IL-10/CD3, IL-10/CD68, and IL-10/CD205/DC-SIGN staining, images were acquired on an Olympus VS110, fluorescence version, with a 100-slide loader and VS-ASW FL 2.4 (build 90535) software; 50 randomly selected, evenly spaced fields were analyzed at 400× magnification.

Splenic architecture allowed for identification of white and red pulp by the absence or presence, respectively, of splenic sinusoids. Specific zones examined within the lymph nodes included the paracortex (T cell area) and B cell follicles and germinal centers. As T cells, B cells, dendritic cells, and macrophages are located in specific microanatomic compartments within spleens or lymph nodes, data are reported for the whole tissue.

Flow-cytometric phenotyping. Multiparameter flow-cytometric analysis was performed to characterize lymphocyte populations in PBMC and tissue cell suspensions. All antibodies were from BD Biosciences (San Jose, CA) unless otherwise stated. T cell subpopulations of $CD3^+$ (clone SP34-2) and $CD4^+$ (clone L200) or $CD8^+$ (clone SK1) T cells were further defined by a marker of apoptosis (caspase 3 [clone C92-605]). Data are

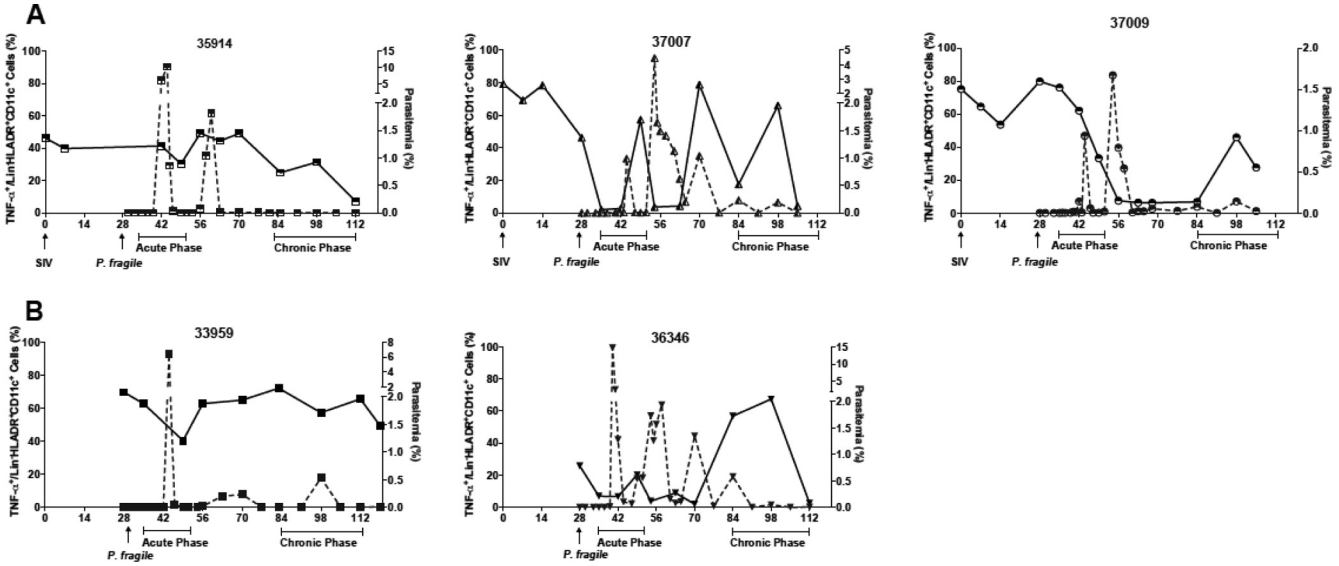

FIG 1 Correlation of peripheral blood parasitemia and myeloid dendritic cell (mDC) TLR4 responsiveness. TLR4 responsiveness (solid line) and parasitemia (dashed line) are shown for individual animals that were coinfected with SIV and *P. fragile* (A) or infected only with *P. fragile* (B). TLR4 responses were measured after *in vitro* stimulation of peripheral blood mononuclear cells with 1 μg/ml lipopolysaccharide (LPS) and subsequent multicolor flow-cytometric analysis. The percentage of TNF-α^+ cells in the total mDC population (Lin^- $CD11c^+$ HLA-DR^+) is shown. Parasitemia is reported as the percentage of infected red blood cells.

recorded as the percentage of caspase 3^+ cells in $CD3^+$ $CD4^+$ or $CD3^+$ $CD8^+$ populations. Frequencies of regulatory T cells (Treg) were quantified by staining with CD3, CD4, CD25 (clone 4E3), and FoxP3 (clone 259D; BioLegend, San Diego, CA) and stained according to the BioLegend protocol. Data are reported as the percentage of $CD25^+$ $FoxP3^+$ cells of the total $CD3^+$ $CD4^+$ population. Peripheral blood Treg percentages were then converted to the total number of Treg per μl of blood based on complete blood count data. Samples were acquired on a FACSAria (BD, San Jose, CA), and data were analyzed using FlowJo software (TreeStar, Ashland, OR).

Statistics. To evaluate the differences in plasma cytokine changes over time between the various infection groups, the slope or change in each of these cytokine levels over time, as well as the change in their ratio, was computed for each animal. For each animal a permutation test was employed to test the hypothesis that the slope was equal to zero. Permutation tests were conducted only when data were available at four or more time points for an animal (R statistical computing software, version 2.14). Because of the small sample sizes, formal statistical comparisons were not conducted between groups of animals.

Expression levels of genes that were measured by TLR PCR array were compared between controls and animals in experimental groups using the online RT^2 Profiler PCR array data analysis software, version 3.5, which includes a statistical analysis component.

RESULTS

Distinct TLR responses of peripheral blood mDC and monocytes. To determine whether altered or dysfunctional responses of Mo/Mph or mDC could contribute to disease exacerbation in SIV-*P. fragile* coinfection, we tested the cytokine response of mDC to the TLR4 ligand lipopolysaccharide (LPS). PBMC from all SIV-*P. fragile*-coinfected animals showed robust TNF-α responses after LPS stimulation (Fig. 1). However, the frequencies of TNF-α-secreting mDC within an individual animal varied considerably throughout the course of infection (Fig. 1A). TLR responses were reduced during acute SIV infection and concurrently or just subsequent to parasitemic episodes. Control of primary parasitemia was associated with normalizing TLR responses, but these appeared to decrease again after secondary parasitemic episodes. These data were indicative of a temporal association between parasitemia and TLR responsiveness of peripheral blood mDC in the earlier stages of infection. Despite the recovery of TNF-α responses, there was a trend toward overall diminished TLR function in chronically SIV-*P. fragile*-coinfected animals compared to preinfection animals (Fig. 1A). A similar pattern of decreased mDC TNF-α responses during parasitemic episodes and response recovery after parasite control was observed in acute *P. fragile*-infected animals. Chronically *P. fragile*-infected animals showed more variable responses. The mDC response in animal 33308 was similar to preinfection levels at the time of euthanasia, while TLR responses fluctuated in the *P. fragile*-infected animal 36346 and were reduced at the time of euthanasia (Fig. 1B). To establish clearly defined trends, larger animal numbers per infection group and more frequent sampling would have been necessary. However, in this initial experiment, TLR responses were assessed only every 7 or 14 days during acute or chronic malaria, respectively. To better characterize changes in mDC function throughout infection, we assessed the response to stimulation with the TLR7/8 agonist R848 and the TLR2 agonist lipomannan (LPM), rationalizing that SIV contains single-stranded RNA (ssRNA), a TLR7/8 agonist, while *Plasmodium* species express TLR2 agonists, e.g., glycosylphosphatidylinositols (35). Furthermore, to assess the quality of the TLR response and its potential impact on adaptive immunity, we measured IL-12, a key cytokine for T helper 1 (Th1) responses, and IL-10, an immunoregulatory cytokine, in addition to TNF-α. This was a retrospective analysis. Due to limited cell availability, only 2 of 3 coinfected animals (35914 and 37009), 2 of 3 *P. fragile*-infected animals (33308 and 33959), and 2 SIV-infected animals could be tested. Time points were selected to represent the day of preinfec-

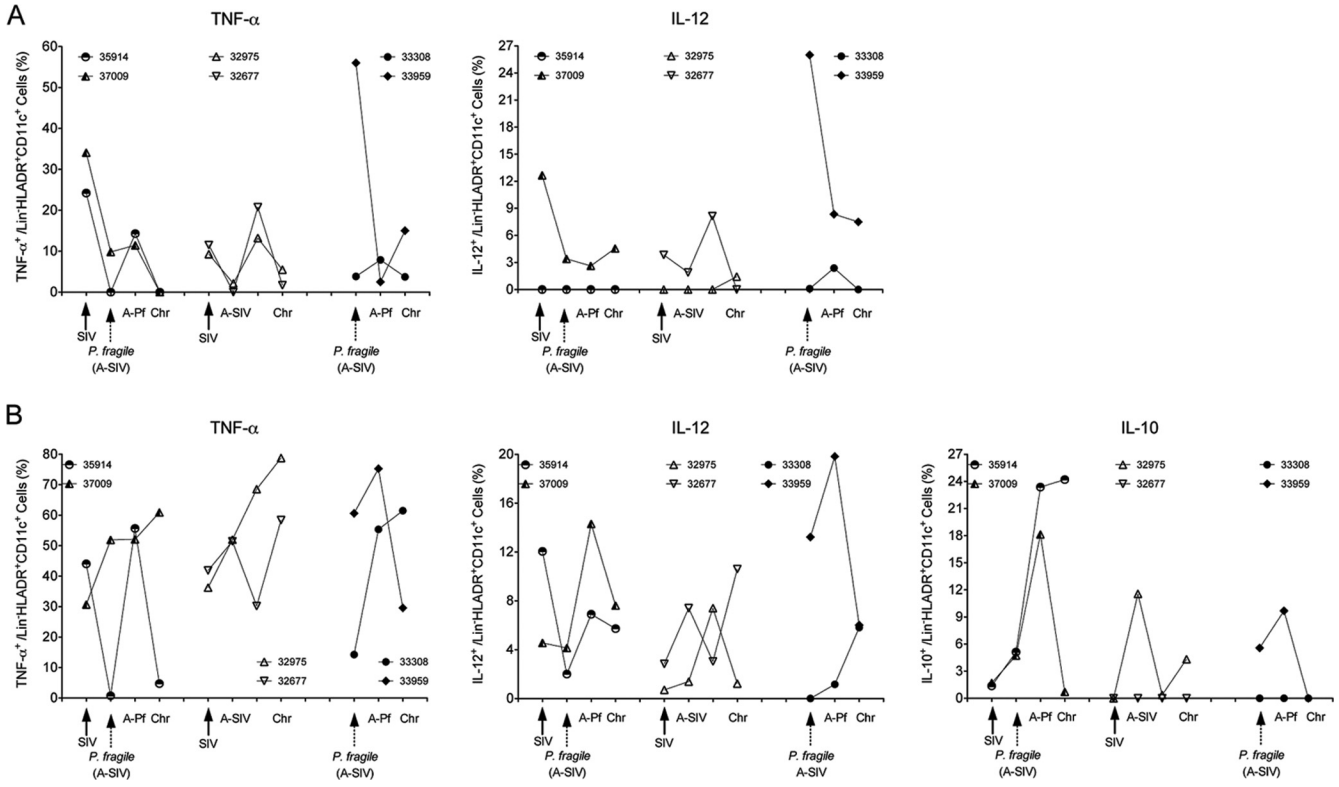

FIG 2 TLR7/8 responses of peripheral blood mDC and monocytes. (A and B) The percentages of cytokine-positive mDC or monocytes, respectively, after *in vitro* stimulation with the TLR7/8 ligand R848. PBMC from animals in the various infections groups were analyzed for the production of TNF-α, IL-12, and IL-10. The experimental groups are ordered in the following order, from left to right on the *x* axis: SIV-*P. fragile* coinfection, SIV infection, and *P. fragile* infection. Individual animals in each group are represented by a specific symbol, as indicated in the graph. Results are shown for the time points corresponding to the time of SIV infection (DPI-SIV 0) or *P. fragile* (DPI-Pf 0/DPI-SIV 28) infection, the time of acute SIV infection (A-SIV and DPI-SIV 28; equivalent to the time of *P. fragile* infection in coinfected animals), acute *P. fragile* infection (A-Pf and DPI-SIV 35 to 49/DPI-Pf 7 to 21), and the chronic phase (Chr) of infection (DPI-SIV 84 to 112/DPI-Pf 42 to 84). See the text for further details.

tion (DPI-SIV 0), *P. fragile* infection (DPI-SIV 28/DPI-Pf 0), acute parasitemia (DPI-SIV 35 to 49 or DPI-Pf 7 to 21), and chronic malaria (DPI-SIV 84 to 112 or DPI-Pf 42 to 84). Responses to LPM and R848 followed a similar trend in an individual animal; however, as LPM responses were relatively low, only R848 responses are reported here. It should be noted that preliminary experiments were performed to confirm that LPS responses using frozen PBMC were comparable to the original assays performed with fresh PBMC (data not shown). Mirroring the results of the initial experiment (Fig. 1), SIV-*P. fragile*-infected animals showed reduced mDC TNF-α responses at DPI-SIV 28, a rebound to baseline at DPI-SIV 42, and a subsequent decrease in TLR responsiveness during chronic infection (Fig. 2A). Only one of the coinfected animals (35914) showed IL-12 responses. In this animal, the frequencies of IL-12-positive mDC declined during SIV infection and remained at this lower level throughout the course of infection. The magnitude of TLR responses in SIV-infected animals followed similar kinetics: cytokine production was reduced during acute infection, with subsequent recovery and decreasing responses during the chronic phase of infection (Fig. 2A). The cytokine response to R848 stimulation in *P. fragile*-infected animals followed a trend similar to that of the LPS data (Fig. 1B). Animal 33308 had increased frequencies of TNF-α- and IL-12-positive mDC during acute parasitemia, but responses during chronic infection were similar to those of preinfection, whereas responses in animal 33959 were reduced during primary parasitemia (Fig. 2A). IL-10 was not induced in peripheral blood mDC of any of the animals.

To explore the potential link between acute parasitemia and temporal loss of mDC function, we extended the analysis to monocytes, because peripheral blood Mo play an active role in the clearance of parasite-infected red blood cells (iRBC) in malaria infection. Overall, the magnitude of the responses to TLR stimulation was higher in Mo than in mDC. Notably, and in contrast to mDC responses, TNF-α responses persisted in one (37009) of the SIV-*P. fragile*-coinfected animals (Fig. 2B). Similarly, frequencies of IL-12-producing Mo in coinfected animals were maintained throughout the course of infection. Furthermore, and contrary to peripheral blood mDC, R848 stimulation of Mo induced not only TNF-α and IL-12 but also IL-10. Frequencies of IL-10-producing Mo in SIV-*P. fragile*-coinfected animals started to rise during acute SIV infection, increased further during acute parasitemia (18 to 25%), and persisted in 1 of the 2 animals (35914) (Fig. 2B). Although IL-10-producing Mo were also detectable in one of the SIV-infected and one of the *P. fragile*-infected animals, the frequencies were lower than those of coinfected animals (Fig. 2B). IL-10 has been shown to promote the differentiation of peripheral Mo toward a macrophage phenotype while simultaneously inhibiting mDC maturation (36–38), and this might explain the observed divergent TLR response patterns in Mo versus mDC.

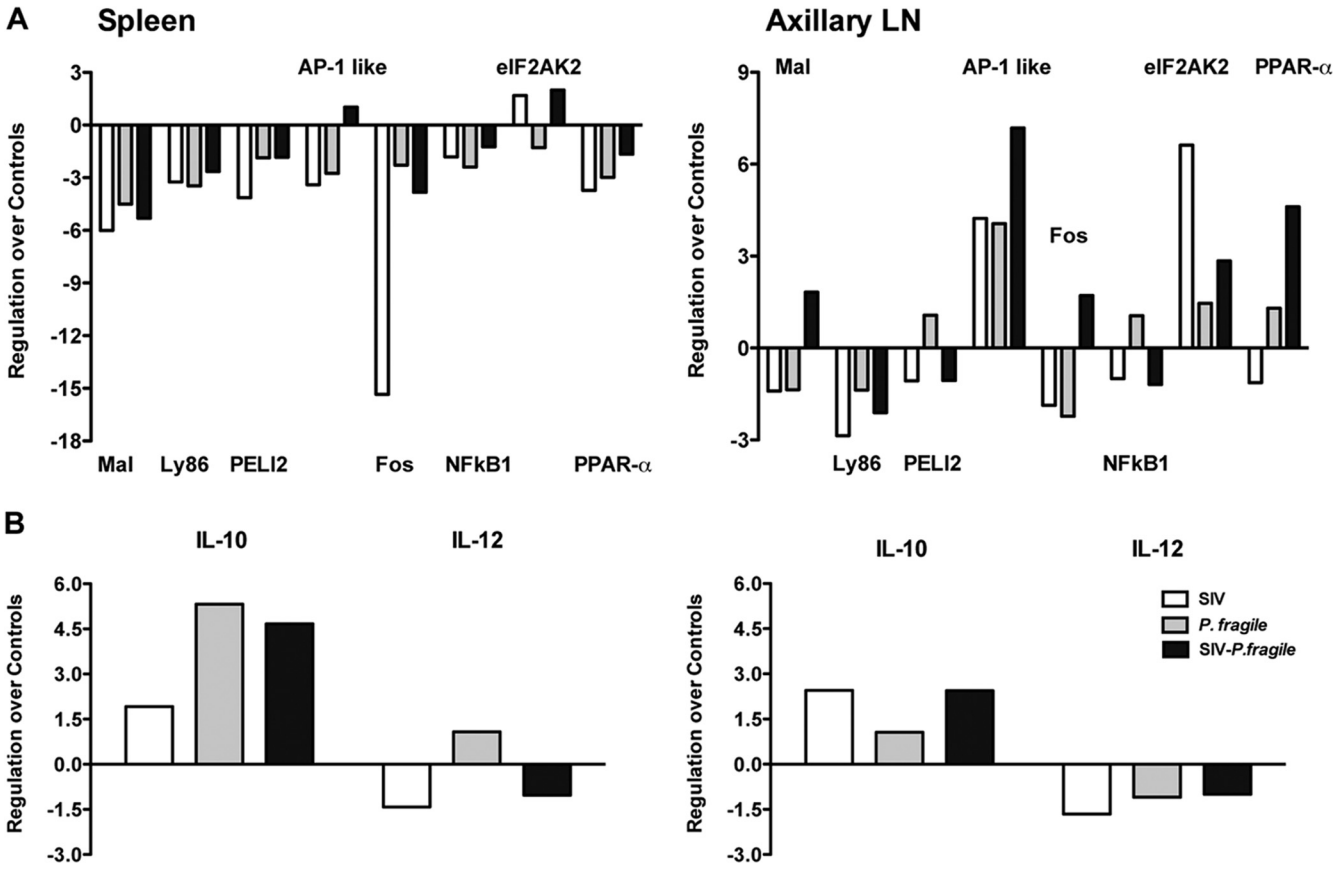

FIG 3 Gene expression of specific TLR signaling molecules in tissues. Spleens and axillary lymph nodes collected at 3 months postinfection were analyzed for mRNA expression of TLR signaling molecules by a TLR PCR array. (A) Average fold regulation for TLR adapter molecules and transcription factors for SIV (empty bars)-infected, *P. fragile* (gray bars)-infected, and SIV-*P. fragile*-coinfected (black bars) animals. Data were analyzed using the manufacturer's online RT^2 Profiler PCR array data analysis software. Changes in mRNA levels are expressed compared to the same mRNA levels in the same tissues collected from three uninfected healthy control animals. (B) Fold regulation for IL-10 and IL-12 mRNA levels in spleens and axillary lymph nodes.

SIV-infected animals maintained Mo TNF-α responses at or slightly above preinfection levels throughout infection (Fig. 2B). The induction of IL-12 by Mo appeared to antagonize induction of IL-10 and vice versa. For example, in animal 32975, frequencies of IL-12-positive Mo were highest at DPI-SIV 35 to 49, when frequencies of IL-10-positive Mo are lowest, but IL-10 induction dominated that of IL-12 during acute and chronic SIV infection (Fig. 2B). In the other SIV-infected animal, IL-12 was more strongly induced in Mo during acute and chronic SIV infection, and IL-10-positive Mo could not be detected at any time. As was observed for mDC responses in the two *P. fragile*-infected animals, animal 33959 showed more robust responses than 33308 (Fig. 2B). The higher and more persistent response might be due to the higher acute parasitemia (8%) in animal 33959 than in animal 33308 (3%) (9).

Thus, there was an apparent dichotomy in the *in vitro* TLR responses of peripheral blood mDC and Mo. Monocytes of SIV-*P. fragile*-coinfected animals appeared to maintain TLR responsiveness throughout the course of infection and produced IL-10 in addition to TNF-α and IL-12.

Altered TLR responses in tissues. Altered innate TLR responses of peripheral blood mDC and Mo in chronic SIV-*P. fragile*-coinfected animals could negatively impact SIV- and/or malaria-specific immunity. Therefore, we tested whether we could detect similar changes in mDC and Mo/Mph function in secondary lymphoid organs, such as spleen and lymph nodes, where adaptive immune responses are initiated. The importance of these tissues is further underlined by their role in SIV and/or *P. fragile* infection. The spleen serves as the primary site for the clearance of parasite-infected red blood cells (39, 40), and lymphadenopathy is a common clinical feature in HIV/SIV infection.

To test whether tissue TLR responses were impaired, we used a rhesus macaque-specific RT^2 PCR TLR signaling array. The TLR adapter molecules PELI2 and Ly86 were downregulated in spleen and axillary lymph nodes of coinfected animals. The mRNA levels of the adapter molecule Mal were reduced in spleen but slightly increased in the axillary lymph nodes of coinfected animals (Fig. 3A). However, similar changes in mRNA levels were observed in SIV- and *P. fragile*-infected animals. In addition, several transcription factors (NF-κB1, fos, and PPAR-α) were downregulated in the spleen of coinfected animals compared to age-matched tissues of uninfected control animals (Fig. 3A). The transcription factors AP-1-like and eIF2AK2 were increased in both spleens and axillary lymph nodes. In fact, in the axillary lymph nodes of coinfected animals, the transcription factors fos and PPAR-α were also induced compared to levels in uninfected controls, suggesting that some TLR responses in chronic SIV-*P. fragile*-coinfected animals is altered in a tissue-specific manner. Consistent with this conclu-

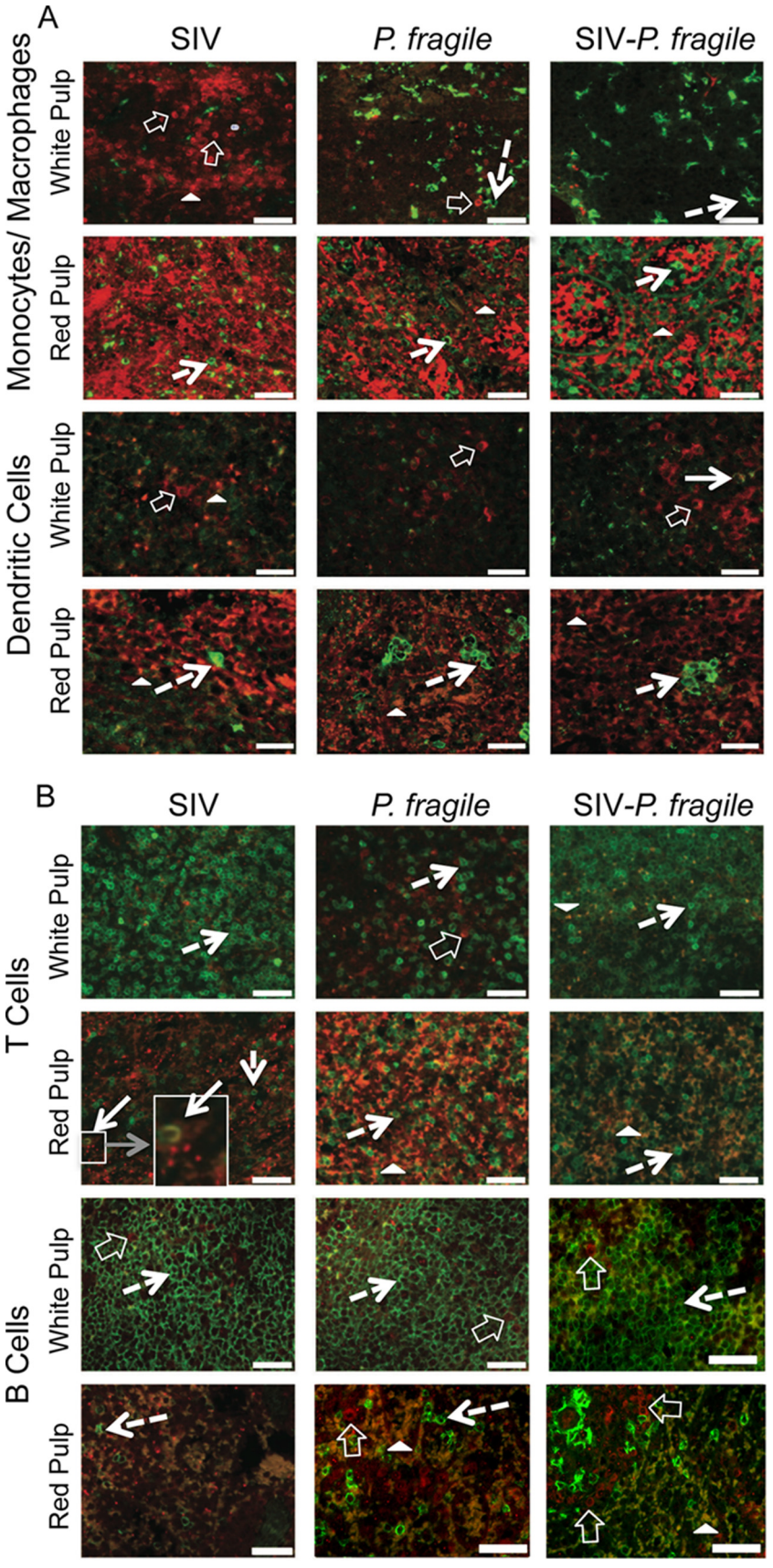
A
SIV
P. fragile
SIV-P. fragile
Monocytes/ Macrophages
White Pulp
Red Pulp
Dendritic Cells
White Pulp
Red Pulp
B
SIV
P. fragile
SIV-P. fragile
T Cells
White Pulp
Red Pulp
B Cells
White Pulp
Red Pulp

sion, SIV-*P. fragile* ($P < 0.006$)- and *P. fragile* ($P < 0.02$)-infected animals, but not SIV-infected animals, showed significantly higher IL-10 mRNA levels in the spleen compared to uninfected controls (Fig. 3B). Although IL-10 mRNA levels were also slightly elevated compared to control animals ($P < 0.02$) in axillary lymph nodes of infected animals, there were no statistically significant differences between the various groups. In contrast to IL-10, IL-12 mRNA levels in both spleens and lymph nodes appeared to be downregulated, but statistically there was no difference in mRNA levels of IL-12p40 between control animals and any of the experimental groups (Fig. 3B). Increased tissue IL-10 mRNA levels concurrent with reduced IL-12p40 mRNA were indicative of an immunosuppressive milieu. This was consistent with the reduced TLR responsiveness of peripheral blood mDC and induction of IL-10 in Mo after *in vitro* TLR stimulation.

Differential IL-10 expression in spleens and lymph nodes. The TLR array was performed with whole-tissue RNA. More conclusive data would have been obtained if purified tissue mDC or Mo/Mph populations were used for the analysis. Therefore, to determine if tissue mDC or Mo/Mph had developed an immunosuppressive phenotype, we enumerated IL-10-positive cells in spleens and axillary lymph nodes by immunofluorescence. Contrary to elevated whole-tissue IL-10 mRNA data, only a few IL-10-producing cells were detectable in the spleens of SIV-*P. fragile*-coinfected animals, and their frequencies were similar to those in *P. fragile*- and SIV-infected animals (Fig. 4 and 5A). Levels of IL-10-positive cells in the spleen were higher in the white pulp, or zone of T and B cell interactions, in SIV-infected and SIV-*P. fragile*-coinfected animals, but they are also present in the red pulp, or zone of/MoMph and erythrocytes, in *P. fragile*-infected animals (Fig. 4). Consistent with this observation, some IL-10-positive Mo/Mph could be detected in the spleen of *P. fragile*-infected animals (Fig. 4 and 5A). Surprisingly, we could not detect any IL-10-producing Mo/Mph or mDC in SIV-*P. fragile*-coinfected animals (Fig. 4A). Instead, the vast majority of IL-10-positive spleen cells were T cells (Fig. 4B). In addition, IL-10-positive B cells were present in the spleen of one of the SIV-*P. fragile*-coinfected animals and in one SIV-infected animal (Fig. 5A). To address the possibility that IL-10-producing T cells represent regulatory T cells (Treg), we analyzed cell populations from spleens and lymph nodes for CD4, CD25, and FoxP3 by flow cytometry. Frequencies of Treg were low in both spleens and axillary lymph nodes of coinfected animals and were not statistically different from Treg frequencies in spleens or lymph nodes of SIV- or *P. fragile*-infected animals (Fig. 5B). Similarly, longitudinal analysis of peripheral blood revealed considerable fluctuations of Treg numbers over time in SIV-*P. fragile*-coinfected and *P. fragile*-infected animals (Fig. 5C and data not shown), and distinct correlations of changes in Treg frequencies and concurrent changes in plasma IL-10 or parasitemia could not be established.

Interestingly, in axillary lymph nodes of SIV-*P. fragile*-coinfected animals, IL-10-positive T cells represented only a minor population among IL-10-positive cells. The majority of IL-10-positive cells in axillary lymph nodes of SIV-*P. fragile*-coinfected animals and of SIV- or *P. fragile*-infected animals expressed an mDC phenotype (Fig. 5A and 6). Despite the lack of IL-10-positive T cells in axillary lymph nodes, IL-10-producing mDC are likely inefficient in the priming of effective SIV and *P. fragile*-specific T cells. Thus, although the phenotype of IL-10-producing cells differed between spleen and lymph nodes, the presence of IL-10-positive mDC in lymph nodes and IL-10-positive T and B cells in spleens was indicative of functionally impaired immune responses.

Immune exhaustion and apoptosis. Defective T cell responses are a sign of immune exhaustion. In HIV infection, immune exhaustion has been linked to persistent immune activation. The endpoint of chronic immune activation for a cell is death via apoptosis (34). Therefore, we hypothesized that SIV-*P. fragile* infection could result in increased apoptosis, and that splenic Mph would be especially prone to apoptosis. Therefore, tissues were costained with caspase 3 and CD68 to detect apoptotic Mo/Mph (Fig. 7A). While not significant, there was a trend toward higher total numbers of apoptotic cells and caspase 3-positive Mo/Mph in SIV-*P. fragile* infection (Fig. 7B).

To determine the potential effect of altered innate responses on adaptive immunity, we measured caspase 3 expression in $CD4^+$ and $CD8^+$ T cells in cell suspensions from spleen and axillary lymph nodes via multicolor flow cytometry (Fig. 7C). Consistent with the immunohistochemistry results, there were no significant differences in the frequencies of caspase 3-positive T cells between the infection groups, although there was a trend toward higher caspase 3-positive T cells in the spleen of coinfected animals. Animals with the highest numbers of caspase 3-positive $CD8^+$ T cells also had the highest percentage of caspase 3-positive $CD4^+$ T cells.

Longitudinal analysis of peripheral blood T cells showed that the percentages of caspase 3-positive $CD4^+$ and $CD8^+$ T cells in SIV-*P. fragile*-coinfected animals varied throughout the course of coinfection (Fig. 8A). There was an initial increase during acute SIV infection, but levels normalized with control of viremia. Subsequent rises in caspase 3-positive T cells seemed to be associated with plasma IL-10 levels (Fig. 8A) and, therefore, likely with parasitemic episodes. Similarly, increased plasma IL-10 levels during acute viremia and primary parasitemia were associated with elevated levels of PD-1, a marker of T cell exhaustion (Fig. 8B). Two of the SIV-*P. fragile*-coinfected animals showed increasing levels of PD-1-positive T cells over time, but in 1 of the 3 coinfected animals (35914), the level of PD-1 expression at the time of euthanasia was similar to preinfection levels (Fig. 8B).

Systemic immune activation versus regulation. T cell exhaustion is observed in many chronic infections due to persistent immune activation. In fact, immune activation is a hallmark of HIV/SIV infection. Theoretically, this inflammatory milieu could be

FIG 4 IL-10 expression in spleen. Immunofluorescence was used to determine the phenotype of IL-10-producing cells in the red and white pulp of the spleen. Representative tissue sections of SIV-, *P. fragile*-, and SIV-*P. fragile*-infected animals at necropsy are shown. Images were stained with IL-10 (red) and the relevant lineage markers (green) for monocyte/macrophages (CD68), dendritic cells (CD205/DC-SIGN), T cells (CD3), or B cells (CD20). Panel A shows images for monocytes/macrophages and dendritic cells, and panel B includes the relevant images for T and B cells. Negative controls were performed via staining with appropriate isotype controls, and images were acquired and analyzed as positively stained sections (Fig. 6). White bars represent 50 μm. Despite the strong autofluorescence of red cells (closed white triangle) in the red pulp of the spleen, IL-10-positive cells could be clearly identified. Single cells positive for IL-10 are indicated by clear white block arrows, and lineage marker-positive cells are pointed out by dashed arrows. The boxed area and its enlargement in the SIV example shows a CD3-positive cell that is also positive for IL-10 (white arrow).

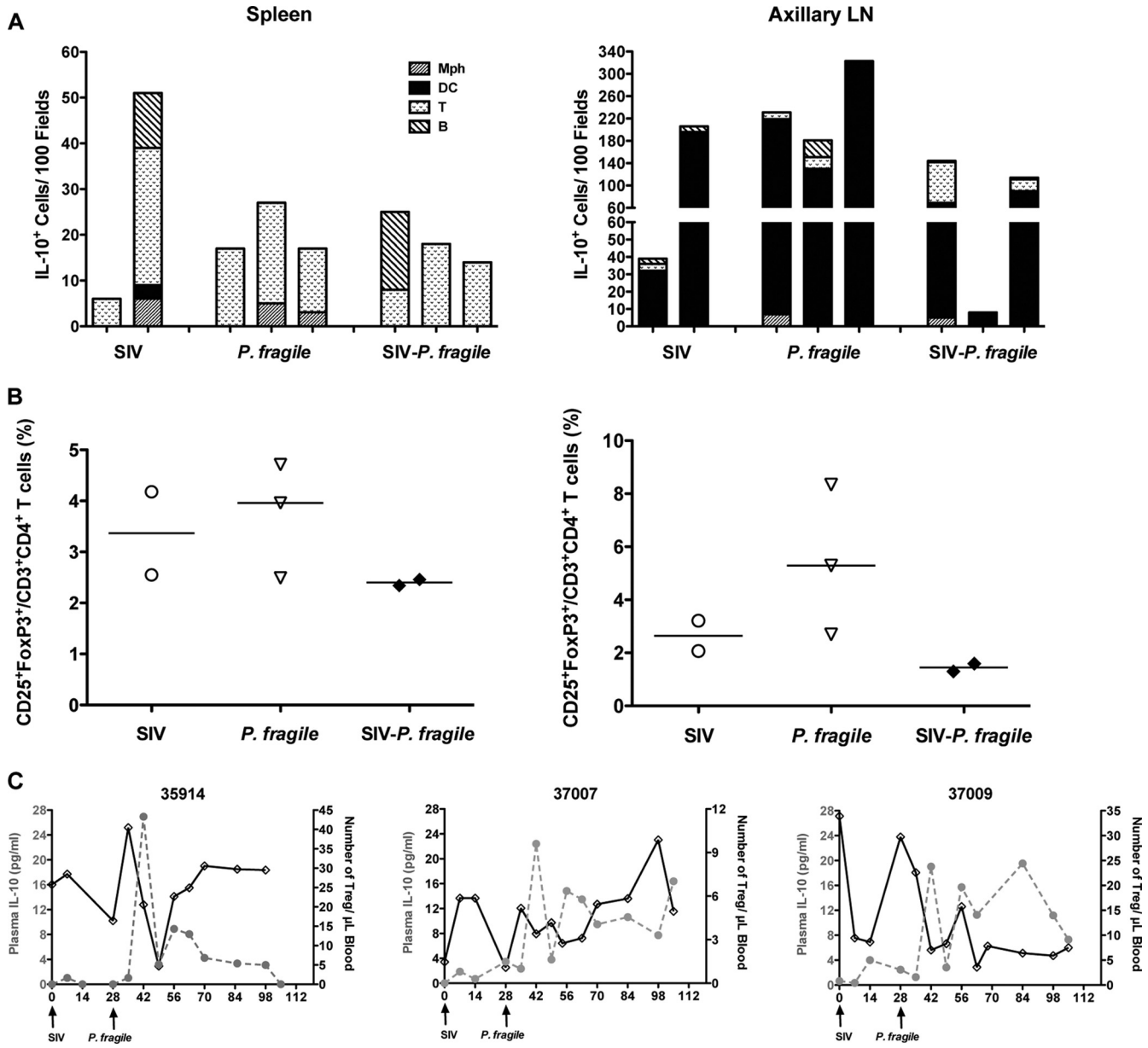

FIG 5 Cellular profile of IL-10-positive cells. (A) Total number of IL-10-positive cells in 100 fields of spleens (left) or axillary lymph nodes (right) of SIV-, *P. fragile*-, and SIV-*P. fragile*-infected animals that were determined by IHC (Fig. 4 and 6). Each bar represents an individual animal. The various patterns within the bars represent the number of Mo/Mph, mDC, T cells, and B cells. (B) Percentage of regulatory T cells within spleen (left) or axillary lymph node (right graph) cell suspensions. Each symbol represents an individual animal. The horizontal bar depicts the median percentage of Tregs within a specific infection group. (C) Longitudinal changes in peripheral blood regulatory T cells (black solid line) of SIV-*P. fragile*-coinfected animals in relation to plasma IL-10 levels (gray dotted line).

counteracted in SIV-*P. fragile*-coinfected animals, because chronic malaria infection leads to persistent levels of hemozoin, a by-product of *Plasmodium* species that is known to induce IL-10. High levels of IL-10, on the other hand, interfere with parasite clearance (15, 41–43), thereby promoting the persistence of malaria antigens that will contribute to increased immune activation. Therefore, it is important to determine the net balance of pro- and anti-inflammatory cytokines. In the current study, we measured plasma IL-10 and IL-12 levels. In fact, systemic plasma IL-10 levels increased during primary parasitemia both in SIV-*P. fragile*- and in *P. fragile*-infected animals but were unaltered in SIV-infected animals (Fig. 9). Although plasma IL-10 levels decreased after acute parasitemia, they persisted above preinfection levels throughout chronic SIV-*P. fragile* and *P. fragile* infection. Altered plasma IL-10 levels appeared to correspond to blood parasitemia levels, suggesting that there is a direct relationship between parasite burden and IL-10 plasma levels *in vivo* (Fig. 9D). Considering that SIV drives immune activation, we tested whether malaria-induced IL-10 plasma levels were associated with suppression of IL-12. IL-12 was chosen as a representative inflammatory cytokine, because higher frequencies of peripheral blood Mo responded to *in vitro* TLR stimulation with IL-10 (15 to 25%) than

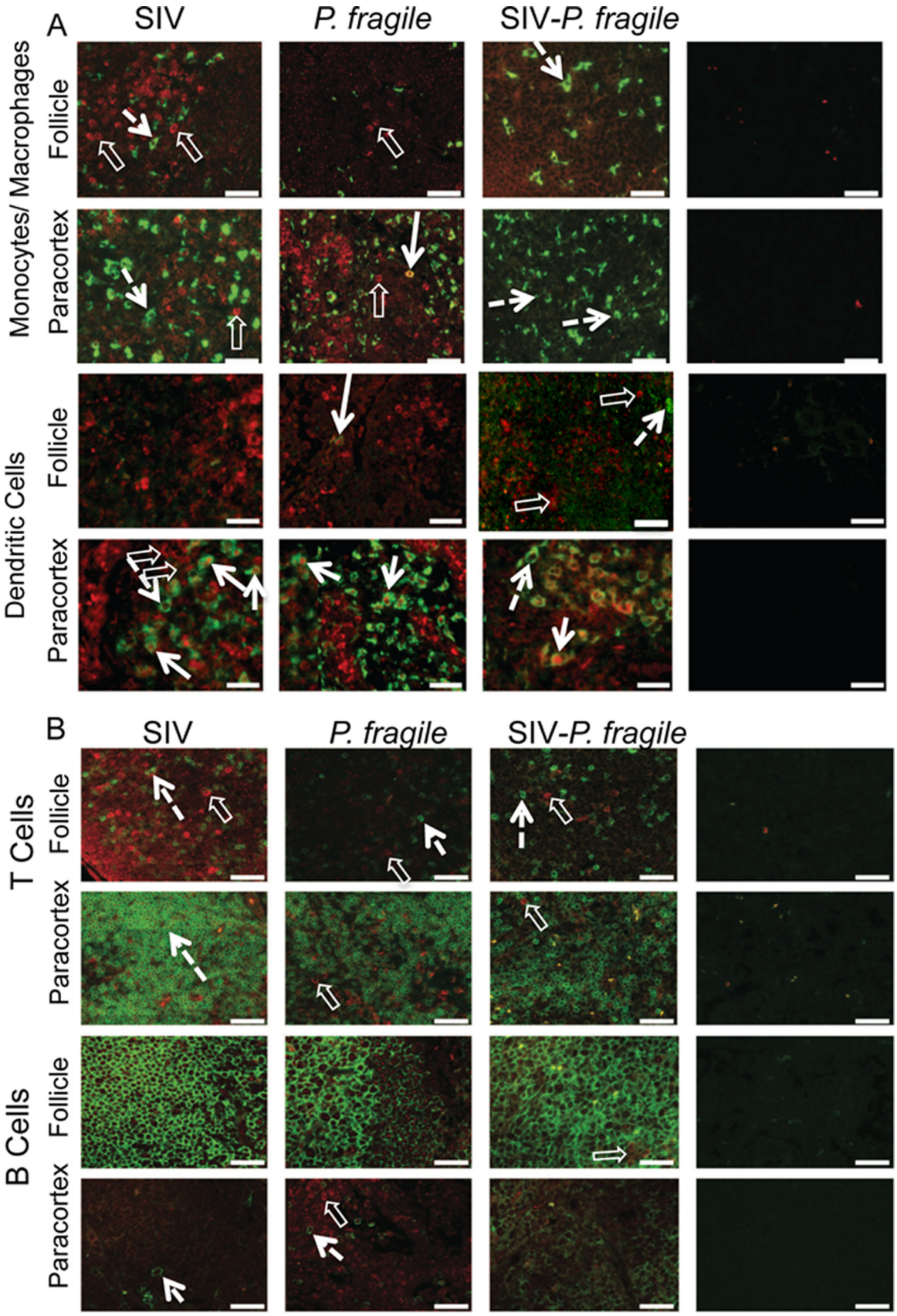

FIG 6 IL-10 expression in axillary lymph nodes. Immunofluorescence was used to determine the phenotype of IL-10-producing cells in the paracortex (T cell zone) and follicle (B cell area) of axillary lymph nodes. Representative tissue sections of SIV-, *P. fragile*-, and SIV-*P. fragile*-infected animals at necropsy are shown. Images show sections stained for IL-10 (red) and Mo/Mph or mDC markers (A) or sections stained for IL-10 and T or B cell markers (B). Single- and double-positive cells are identified as described in the legend to Fig. 4.

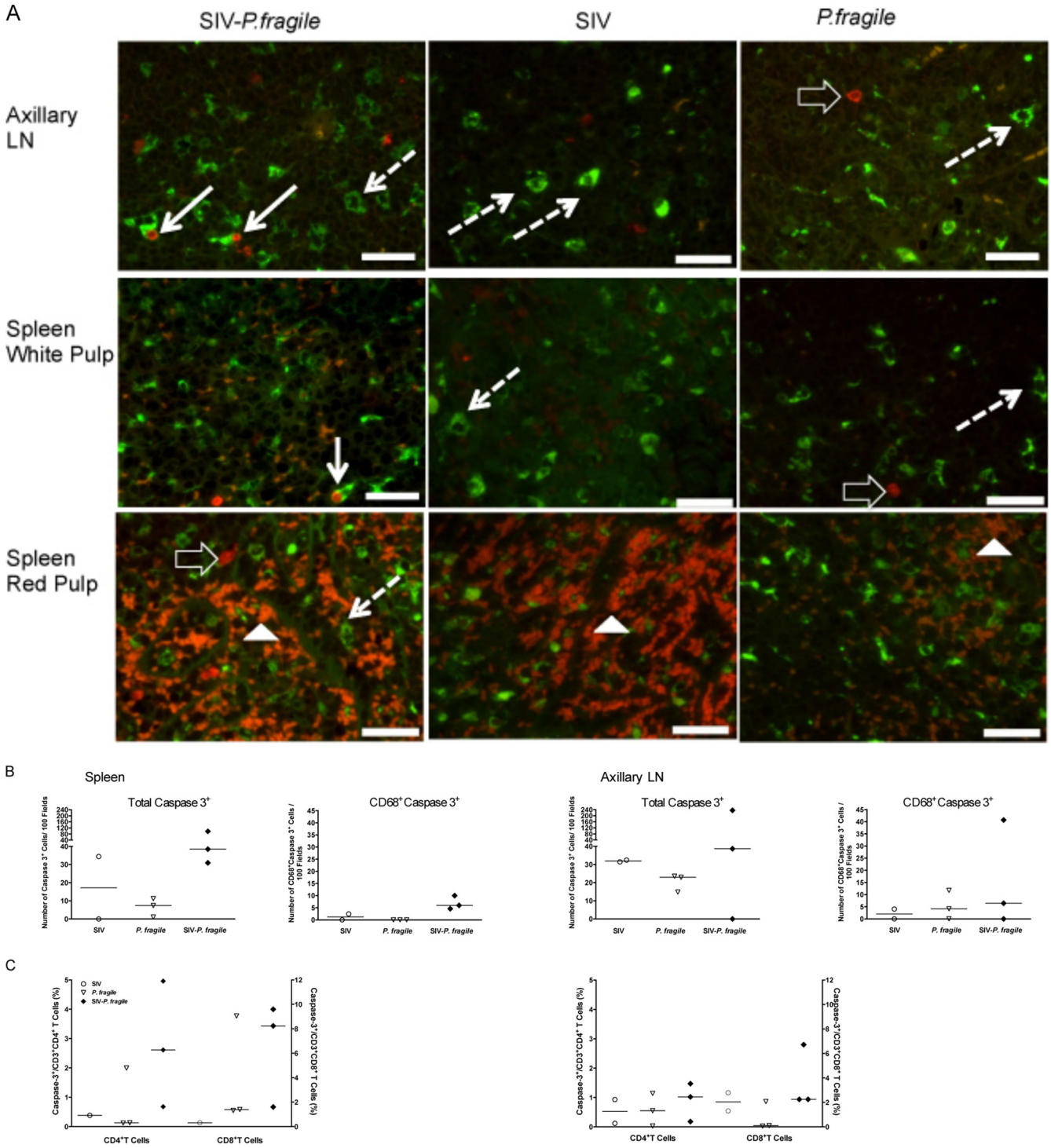

FIG 7 Apoptosis in lymphoid tissues. (A) Representative examples of tissue sections stained for caspase 3 (red) and CD68 (green) in axillary lymph nodes and spleens of SIV-, *P. fragile*-, and SIV-*P. fragile*-infected animals. Cells double positive for CD68 and caspase 3 in the axillary LN and the white pulp of SIV-*P. fragile*-infected animals are marked by a solid white arrow. Examples of Mo/Mph staining positive for CD68 are indicated by dashed white arrows, and representative caspase 3-positive cells are highlighted by the open arrows. Note that there is significant autofluorescence by red blood cells (color is more orange than that of red caspase 3-positive cells) within the red pulp; examples are shown by white filled triangles. (B) Summary of the data obtained by IHC analysis. Reported are the total frequencies of caspase 3-positive cells within a tissue and the frequencies of CD68-positive, caspase 3-positive cells (each per 100 fields analyzed). Each symbol represents an individual animal, and horizontal bars show the median values for all animals within one experimental group. (C) Flow-cytometric analysis of spleen and axillary lymph node cell suspensions for caspase 3-positive CD4 and CD8 T cells. Note that we only had spleen cells from one SIV-infected animal available to perform this analysis.

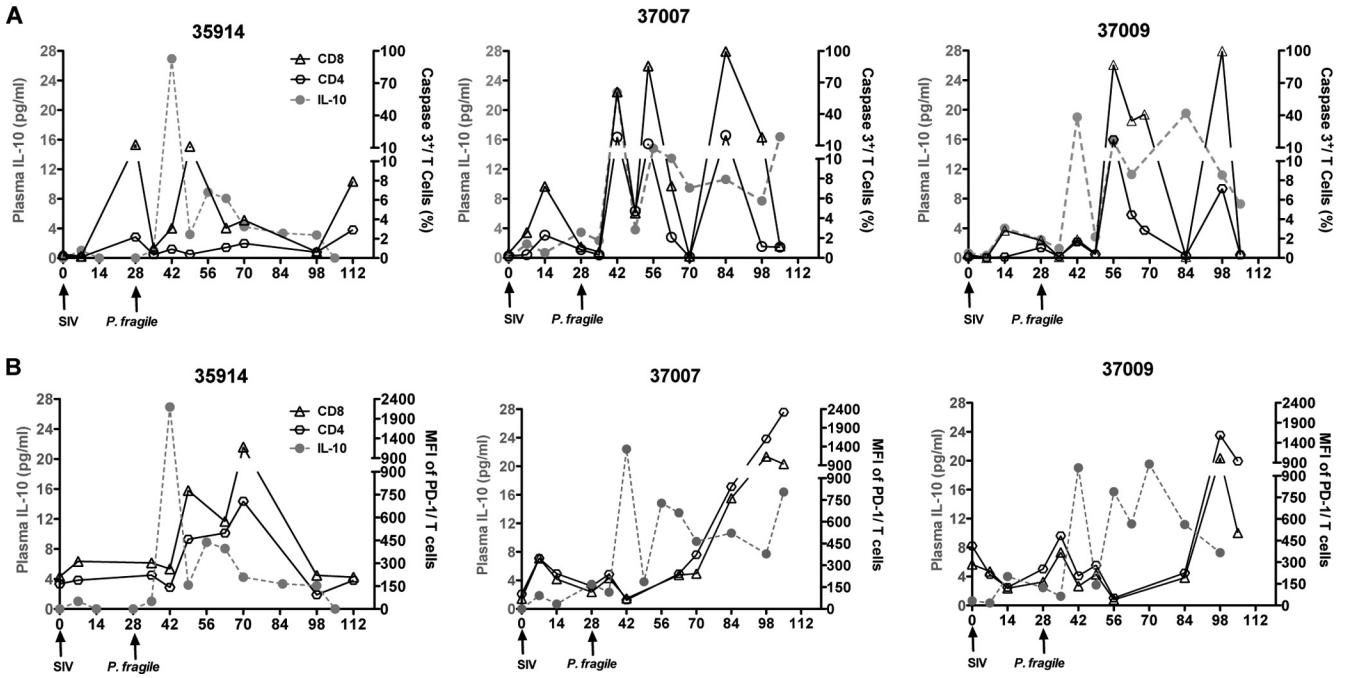

FIG 8 Apoptosis and T cell exhaustion in peripheral blood. Longitudinal blood samples of SIV-*P. fragile*-coinfected animals were analyzed for caspase 3 (A) and PD-1 (B) expression by flow-cytometric analysis. Shown are the percentages of caspase 3- or PD-1-positive CD3 T cells within an individual animal over time in relation to plasma IL-10 levels (gray dotted line). Data are reported for both CD4 (open circle) and CD8 (open triangle) T cells.

with IL-12 (10 to 15%) production (Fig. 2B), and IL-12 mRNA levels were slightly suppressed in tissues of coinfected animals. Interestingly, plasma IL-12 levels of SIV-*P. fragile*-coinfected animals increased throughout the course of infection (Fig. 9A). Plasma IL-12 levels started to rise after SIV infection and decreased in response to acute parasitemia when plasma IL-10 levels were high, but then they steadily increased again once primary parasitemia was controlled. A similar trend toward overall increased plasma IL-12 levels during later time points in chronic infection compared to preinfection was observed in SIV-infected animals (Fig. 9B). Conversely, in 2 of 3 *P. fragile* animals, plasma IL-12 levels remained at preinfection levels. In the third *P. fragile*-infected animal, plasma IL-12 levels fluctuated but also had reached preinfection levels at the time of euthanasia (Fig. 9C). Thus, although definite conclusions cannot be drawn due to the small animal numbers, the rise in plasma IL-12 appeared to be primarily a response to SIV infection, while parasitemia appeared to determine plasma IL-10 levels (Fig. 9D).

To confirm the significance of these findings, the change in cytokine levels over time was examined for each animal (Fig. 9A to C). All three coinfected animals had significant positive increases in IL-12 ($P \leq 0.01$ for each animal), whereas only one of the SIV-infected animals and none of the *P. fragile*-infected animals did. Two of the three coinfected animals had marginally significant positive increases in IL-10 ($P \leq 0.10$), but none of the SIV-infected or *P. fragile*-infected animals did. Similarly, two of the three coinfected animals had marginally significant positive increases in the IL-12/IL-10 ratio ($P \leq 0.10$), whereas one of the SIV-infected animals and none of the *P. fragile*-infected animals did. These data suggest that the systemic immune response in coinfected animals was shifted toward chronic immune activation.

DISCUSSION

The current study describes the interplay between malaria parasite-induced immune regulation and SIV-driven inflammation in SIV-*P. fragile*-coinfected macaques. Peripheral blood responses revealed a dysregulation of innate immune responses in coinfected animals. Specifically, we demonstrate that parasitemic episodes are associated with increased plasma IL-10 levels. IL-10 is a key cytokine in malaria. Acute malaria results in an inflammatory response that is necessary for parasite clearance (14). We have previously confirmed that our rhesus macaque SIV-*P. fragile* coinfection model recapitulates this response (9). To prevent immunopathology, IL-10 is induced immediately following acute parasitemia (14). At the same time, excess IL-10 can inhibit the induction of effective antimalaria immunity (44–47). Monocytes exposed to hemozoin for prolonged times will downregulate Cox-2 and IL-12 and increase IL-10 production (44–47), and the continued activation of monocytes will eventually result in bone marrow suppression (41, 44, 47–52). In addition, Hz can also interfere with mDC maturation (21, 22, 47, 50, 53). Although altered function of monocytes and mDC has been described extensively in severe and chronic malaria infection (15, 36, 41, 44, 51, 54–57), in the current study immune dysfunction was established in coinfected animals that were clinically stable without exceedingly high parasitemia in the 3-month study period.

Our data demonstrate that *in vitro* TLR responses of peripheral blood mDC are altered in SIV-*P. fragile*-coinfected animals. SIV- or *P. fragile*-infected animals had reduced TLR responses during acute SIV infection and acute parasitemic episodes, respectively, but these recovered after the initial control of infection. In contrast, despite a similar trend of transiently suppressed TNF-α responses and subsequent normalization, frequencies of TNF-α-

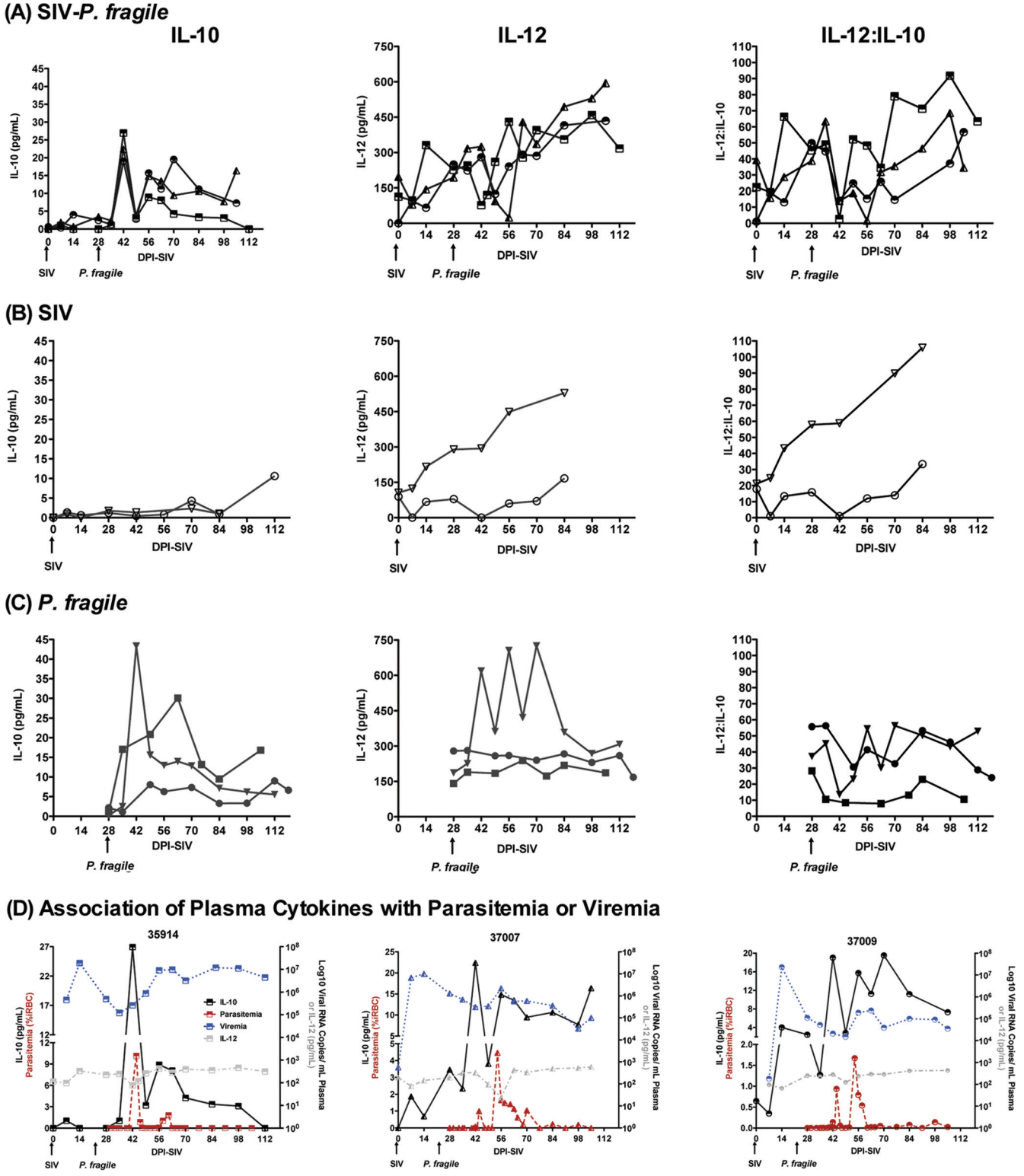

FIG 9 Plasma cytokine levels. Plasma IL-10 (left column) and IL-12 (middle column) levels were determined in longitudinally collected plasma samples by ELISA of SIV-*P. fragile* (A)-, SIV (B)-, or *P. fragile* (C)-infected animals. Individual animals are denoted by different symbols. The ratio of plasma IL-12 to IL-10 (with cytokine-negative samples being assigned a value of 5 pg/ml, the limit of detection) are shown in the right column. (D) The temporal association between plasma viremia or parasitemia with plasma IL-10 or IL-12 levels.

producing mDC continuously declined in SIV-*P. fragile*-coinfected animals. This loss of proinflammatory function of mDC was not replaced by an immunoregulatory response. At no time did we detect IL-10 production by peripheral blood mDC in response to *in vitro* TLR stimulation. Contrary to mDC, peripheral blood Mo of SIV-*P. fragile*-infected animals were able to maintain or even slightly increase TLR responses throughout infection and produced IL-10 in addition to TNF-α and IL-12. Interestingly, IL-10 has been implicated in promoting the differentiation of peripheral Mo toward a macrophage phenotype while simultaneously inhibiting mDC maturation (36–38, 58). The potential role of IL-10 in the suppression of mDC function in SIV-*P. fragile*-coinfected animals was supported by the fact that the loss of peripheral blood mDC function was temporarily associated with parasitemia. In fact, we found that periods of high parasitemia coincided with periods of elevated plasma IL-10 levels in *P. fragile* and SIV-*P. fragile* infections, further suggesting that IL-10 contributed to altered mDC function in blood. In contrast, SIV-infected animals did not show increased plasma IL-10 levels during the 3-month study period. Our data are reminiscent of human HIV and nonhuman primate SIV studies demonstrating that monocytes show increased turnover and hyperresponsiveness, while mDC become more immunosuppressive as infection progresses (25, 58–63).

As parasitemia-induced IL-10 seemed to drive mDC dysfunction, we tested whether this was also reflected in an immunosuppressive milieu in tissues. The spleen, as the major site for the clearance of parasite-infected red blood cells, did have elevated IL-10 mRNA levels in animals infected with *P. fragile* only or in SIV-*P. fragile*-coinfected animals. Hemozoin-loaded mDC and Mo/Mph preferentially accumulate in the red pulp of the spleen (39, 40, 44, 47, 50). Similarly, we had noticed hemozoin deposits in spleens of coinfected animals (9). Based on these data and the fact that there was evidence of altered TLR signaling in the spleen, we expected to detect numerous IL-10-positive Mo/Mph and mDC in the spleen. Surprisingly, the majority of IL-10-positive cells in spleens were neither monocyte/macrophages nor mDC. It is feasible that functionally impaired monocytes or mDC undergo apoptosis, and while we found some evidence of increased apoptosis in the spleens of coinfected animals, this trend was not statistically significant. The majority of IL-10-positive spleen cells represented T cells. This finding is consistent with a recent study in the mouse model of *P. chabaudi* infection that identified CD4 T cells as the main producers of IL-10 in acute malaria (17). We did not find evidence of expansion of a regulatory IL-10-positive T cell population in tissues or blood of coinfected animals. Interestingly, Lamb et al. demonstrated that CD4 T cells in *P. chabaudi*-infected mice can produce both IL-10 and IFN-γ, indicative of impaired effector T cell function (17). Future studies need to determine whether a preferential accumulation of Mo/Mph and mDC in the red pulp of SIV-*P. fragile*-coinfected and *P. fragile*-infected animals prevented optimal priming of effector T cells in the white pulp (52).

It should be noted that the frequencies and the phenotype of IL-10-positive cells did not differ between SIV-*P. fragile*-coinfected animals and animals infected only with SIV or *P. fragile* only, suggesting that both SIV and *P. fragile* contributed to the induction of IL-10 in tissues. Furthermore, IL-10 was detected not only in the spleen but also in lymph nodes. In fact, lymph nodes showed much higher frequencies of IL-10-positive cells than spleens. This result was contrary to the IL-10 mRNA data, for which we had observed elevated levels in spleens but not lymph nodes. This discrepancy might be due to the fact that whole tissue was used in the PCR TLR arrays, and we did not normalize responses to tissue cell numbers. More importantly, the phenotype of IL-10-positive cells in axillary lymph nodes differed from that in the spleen. However, this was true for all infection groups; thus, this phenomenon might be more a reflection of the function of the specific organ in host immunity than of a response to a specific pathogen. Therefore, IL-10-driven immunosuppression in tissues was not a specific characteristic of SIV-*P. fragile* coinfection. The vast majority of IL-10-positive cells in lymph nodes represented mDC. We predict that these IL-10-positive mDC in lymph nodes have diminished ability to activate an effective immune response to SIV and malaria (23, 64). However, we did not measure SIV- or malaria-specific T cell responses in the current study. Studies with larger numbers of animals are needed to resolve this question.

In blood, plasma IL-10 was clearly the result of parasite infection, because SIV-infected animals did not show elevated plasma IL-10. In contrast, SIV infection, but not *P. fragile* infection, led to an increase in plasma IL-12. This was consistent with our previous study, in which we demonstrated that primary parasitemia was associated with marked increases in activated CD4 T cells and elevated plasma levels of nitric oxide and proinflammatory cytokines (9). In SIV-*P. fragile*-coinfected animals, the continuously rising IL-12 plasma levels in the face of constant IL-10 levels resulted in a net response that was shifted toward immune activation instead of immune regulation. Persistent immune activation in coinfection is likely to result in increased morbidity and potentially mortality. This conclusion is supported by an earlier study showing that an increased TNF-α/IL-10 ratio is HIV-malaria infection is associated with more severe pathogenesis outcomes (65). It is likely that SIV-induced immune activation is exacerbated by *P. fragile* infection, because large amounts of parasite antigens are released during the process of parasite clearance in the spleen, promoting chronic activation and subsequent immune exhaustion. Consistent with this idea, we observed increased frequencies of total apoptotic cells in splenic tissue from coinfected animals. Furthermore, parasitemia and systemic IL-10 levels were associated with concurrent changes in the frequencies of T cells expressing PD-1, a negative regulator of T cell activation (29). Thus, both *P. fragile* and SIV infection contributed to enhanced immune activation in coinfected animals. We predict that the increased load of both SIV and malaria antigens exacerbates the chronic immune activation that is a hallmark of HIV and SIV infection (29, 31, 66, 67) and will prevent the development of effective antimalaria immunity, because an immunoregulatory response is necessary to sustain a chronic malaria infection and to develop partial immunity to future reinfections with malaria (19, 20, 68, 69). More detailed studies are needed to define which effects on chronic immune stimulation in coinfection are specific for parasite versus viral antigens.

The current study demonstrates the development of dysfunctional innate immune responses in peripheral blood of SIV-*P. fragile*-coinfected animals compared to responses of animals infected only with SIV or *P. fragile*. Altered innate immune responses were manifested relatively early during coinfection; thus, they are likely to have a profound effect on the development of adaptive immunity. This conclusion was supported by numerous IL-10-positive mDC and T cells in lymph nodes and spleen, re-

spectively, and by signs of T cell exhaustion and apoptosis. Although no causative relationships could be established in the current study, both SIV-driven inflammation and parasite-induced IL-10 seem to contribute to impaired immunity. The data presented here are consistent with data observed in HIV-*P. falciparum* infection in humans; therefore, despite not being conclusive due to the small animal numbers and the retrospective nature of the study, they will serve as the basis for more thorough studies with larger animal numbers per group and longer follow-up to dissect the specific interactions of SIV and malaria parasites and their effect on host immunity.

ACKNOWLEDGMENTS

This work was supported by grant R21 AI077373 (NIH/NIAID) to K.A., the California National Primate Research Center Base Funding Grant P510D011107 (NIH/NCRR), and the Center for AIDS Research (CFAR) at UNC Chapel Hill (NIH/NIAID grant P30 AI050410).

We are especially grateful for the support and advice of Frank Ventimiglia at the UC Davis-CNPRC Computational Imaging Core.

REFERENCES

1. **French N, Nakiyingi J, Lugada E, Watera C, Whitworth JA, Gilks CF.** 2001. Increasing rates of malarial fever with deteriorating immune status in HIV-1-infected Ugandan adults. AIDS **15:**899–906.
2. **Grimwade K, French N, Mbatha DD, Zungu DD, Dedicoat M, Gilks CF.** 2004. HIV infection as a cofactor for severe falciparum malaria in adults living in a region of unstable malaria transmission in South Africa. AIDS **18:**547–554.
3. **Hoffman IF, Jere CS, Taylor TE, Munthali P, Dyer JR, Wirima JJ, Rogerson SJ, Kumwenda N, Eron JJ, Fiscus SA, Chakraborty H, Taha TE, Cohen MS, Molyneux ME.** 1999. The effect of Plasmodium falciparum malaria on HIV-1 RNA blood plasma concentration. AIDS **13:**487–494.
4. **Korenromp EL, Williams BG, de Vlas SJ, Gouws E, Gilks CF, Ghys PD, Nahlen BL.** 2005. Malaria attributable to the HIV-1 epidemic, sub-Saharan Africa. Emerg. Infect. Dis. **11:**1410–1419.
5. **Kublin JG, Patnaik P, Jere CS, Miller WC, Hoffman IF, Chimbiya N, Pendame R, Taylor TE, Molyneux ME.** 2005. Effect of Plasmodium falciparum malaria on concentration of HIV-1-RNA in the blood of adults in rural Malawi: a prospective cohort study. Lancet **365:**233–240.
6. **Mount AM, Mwapasa V, Elliott SR, Beeson JG, Tadesse E, Lema VM, Molyneux ME, Meshnick SR, Rogerson SJ.** 2004. Impairment of humoral immunity to Plasmodium falciparum malaria in pregnancy by HIV infection. Lancet **363:**1860–1867.
7. **Slutsker L, Marston BJ.** 2007. HIV and malaria: interactions and implications. Curr. Opin. Infect. Dis. **20:**3–10.
8. **Van Geertruyden JP, Mulenga M, Chalwe V, Michael N, Moerman F, Mukwamataba D, Colebunders R, D'Alessandro U.** 2009. Impact of HIV-1 infection on the hematological recovery after clinical malaria. J. Acquir. Immune Defic. Syndr. **50:**200–205.
9. **Trott KA, Chau JY, Hudgens MG, Fine J, Mfalila CK, Tarara RP, Collins WE, Sullivan J, Luckhart S, Abel K.** 2011. Evidence for an increased risk of transmission of simian immunodeficiency virus and malaria in a rhesus macaque coinfection model. J. Virol. **85:**11655–11663.
10. **Abu-Raddad LJ, Patnaik P, Kublin JG.** 2006. Dual infection with HIV and malaria fuels the spread of both diseases in sub-Saharan Africa. Science **314:**1603–1606.
11. **Kapiga SH, Bang H, Spiegelman D, Msamanga GI, Coley J, Hunter DJ, Fawzi WW.** 2002. Correlates of plasma HIV-1 RNA viral load among HIV-1-seropositive women in Dar es Salaam, Tanzania. J. Acquir. Immune Defic. Syndr. **30:**316–323.
12. **Franklin BS, Parroche P, Ataide MA, Lauw F, Ropert C, de Oliveira RB, Pereira D, Tada MS, Nogueira P, da Silva LH, Bjorkbacka H, Golenbock DT, Gazzinelli RT.** 2009. Malaria primes the innate immune response due to interferon-gamma induced enhancement of toll-like receptor expression and function. Proc. Natl. Acad. Sci. U. S. A. **106:**5789–5794.
13. **Artavanis-Tsakonas K, Riley EM.** 2002. Innate immune response to malaria: rapid induction of IFN-gamma from human NK cells by live Plasmodium falciparum-infected erythrocytes. J. Immunol. **169:**2956–2963.
14. **Artavanis-Tsakonas K, Tongren JE, Riley EM.** 2003. The war between the malaria parasite and the immune system: immunity, immunoregulation and immunopathology. Clin. Exp. Immunol. **133:**145–152.
15. **Stevenson MM, Riley EM.** 2004. Innate immunity to malaria. Nat. Rev. Immunol. **4:**169–180.
16. **Stevenson MM, Urban BC.** 2006. Antigen presentation and dendritic cell biology in malaria. Parasite Immunol. **28:**5–14.
17. **Freitas do Rosario AP, Lamb T, Spence P, Stephens R, Lang A, Roers A, Muller W, O'Garra A, Langhorne J.** 2012. IL-27 promotes IL-10 production by effector Th1 CD4+ T cells: a critical mechanism for protection from severe immunopathology during malaria infection. J. Immunol. **188:**1178–1190.
18. **Loharungsikul S, Troye-Blomberg M, Amoudruz P, Pichyangkul S, Yongvanitchit K, Looareesuwan S, Mahakunkijcharoen Y, Sarntivijai S, Khusmith S.** 2008. Expression of toll-like receptors on antigen-presenting cells in patients with falciparum malaria. Acta Trop. **105:**10–15.
19. **Perry JA, Olver CS, Burnett RC, Avery AC.** 2005. Cutting edge: the acquisition of TLR tolerance during malaria infection impacts T cell activation. J. Immunol. **174:**5921–5925.
20. **Sanni LA, Jarra W, Li C, Langhorne J.** 2004. Cerebral edema and cerebral hemorrhages in interleukin-10-deficient mice infected with Plasmodium chabaudi. Infect. Immun. **72:**3054–3058.
21. **Bettiol E, Carapau D, Galan-Rodriguez C, Ocana-Morgner C, Rodriguez A.** 2010. Dual effect of Plasmodium-infected erythrocytes on dendritic cell maturation. Malar. J. **9:**64.
22. **Elliott SR, Spurck TP, Dodin JM, Maier AG, Voss TS, Yosaatmadja F, Payne PD, McFadden GI, Cowman AF, Rogerson SJ, Schofield L, Brown GV.** 2007. Inhibition of dendritic cell maturation by malaria is dose dependent and does not require Plasmodium falciparum erythrocyte membrane protein 1. Infect. Immun. **75:**3621–3632.
23. **Millington OR, Di Lorenzo C, Phillips RS, Garside P, Brewer JM.** 2006. Suppression of adaptive immunity to heterologous antigens during Plasmodium infection through hemozoin-induced failure of dendritic cell function. J. Biol. **5:**5.
24. **Sabado RL, Babcock E, Kavanagh DG, Tjomsland V, Walker BD, Lifson JD, Bhardwaj N, Larsson M.** 2007. Pathways utilized by dendritic cells for binding, uptake, processing and presentation of antigens derived from HIV-1. Eur. J. Immunol. **37:**1752–1763.
25. **Sabado RL, O'Brien M, Subedi A, Qin L, Hu N, Taylor E, Dibben O, Stacey A, Fellay J, Shianna KV, Siegal F, Shodell M, Shah K, Larsson M, Lifson J, Nadas A, Marmor M, Hutt R, Margolis D, Garmon D, Markowitz M, Valentine F, Borrow P, Bhardwaj N.** 2010. Evidence of dysregulation of dendritic cells in primary HIV infection. Blood **116:**3839–3852.
26. **Wonderlich ER, Wijewardana V, Liu X, Barratt-Boyes SM.** 2013. Virus-encoded TLR ligands reveal divergent functional responses of mononuclear phagocytes in pathogenic simian immunodeficiency virus infection. J. Immunol. **190:**2188–2198.
27. **Muthumani K, Hwang DS, Choo AY, Mayilvahanan S, Dayes NS, Thieu KP, Weiner DB.** 2005. HIV-1 Vpr inhibits the maturation and activation of macrophages and dendritic cells in vitro. Int. Immunol. **17:**103–116.
28. **Olivetta E, Pietraforte D, Schiavoni I, Minetti M, Federico M, Sanchez M.** 2005. HIV-1 Nef regulates the release of superoxide anions from human macrophages. Biochem. J. **390:**591–602.
29. **Day CL, Kaufmann DE, Kiepiela P, Brown JA, Moodley ES, Reddy S, Mackey EW, Miller JD, Leslie AJ, DePierres C, Mncube Z, Duraiswamy J, Zhu B, Eichbaum Q, Altfeld M, Wherry EJ, Coovadia HM, Goulder PJ, Klenerman P, Ahmed R, Freeman GJ, Walker BD.** 2006. PD-1 expression on HIV-specific T cells is associated with T-cell exhaustion and disease progression. Nature **443:**350–354.
30. **Ford ES, Greenwald JH, Richterman AG, Rupert A, Dutcher L, Badralmaa Y, Natarajan V, Rehm C, Hadigan C, Sereti I.** 2010. Traditional risk factors and D-dimer predict incident cardiovascular disease events in chronic HIV infection. AIDS **24:**1509–1517.
31. **Khaitan A, Unutmaz D.** 2011. Revisiting immune exhaustion during HIV infection. Curr. HIV/AIDS Rep. **8:**4–11.
32. **Velu V, Titanji K, Zhu B, Husain S, Pladevega A, Lai L, Vanderford TH, Chennareddi L, Silvestri G, Freeman GJ, Ahmed R, Amara RR.** 2009.

Enhancing SIV-specific immunity in vivo by PD-1 blockade. Nature **458:** 206–210.
33. **Blackburn SD, Wherry EJ.** 2007. IL-10, T cell exhaustion and viral persistence. Trends Microbiol. **15:**143–146.
34. **Wherry EJ, Ha SJ, Kaech SM, Haining WN, Sarkar S, Kalia V, Subramaniam S, Blattman JN, Barber DL, Ahmed R.** 2007. Molecular signature of CD8+ T cell exhaustion during chronic viral infection. Immunity **27:**670–684.
35. **Krishnegowda G, Hajjar AM, Zhu J, Douglass EJ, Uematsu S, Akira S, Woods AS, Gowda DC.** 2005. Induction of proinflammatory responses in macrophages by the glycosylphosphatidylinositols of Plasmodium falciparum: cell signaling receptors, glycosylphosphatidylinositol (GPI) structural requirement, and regulation of GPI activity. J. Biol. Chem. **280:** 8606–8616.
36. **Chang KH, Stevenson MM.** 2004. Malarial anaemia: mechanisms and implications of insufficient erythropoiesis during blood-stage malaria. Int. J. Parasitol. **34:**1501–1516.
37. **Chang WL, Baumgarth N, Eberhardt MK, Lee CY, Baron CA, Gregg JP, Barry PA.** 2007. Exposure of myeloid dendritic cells to exogenous or endogenous IL-10 during maturation determines their longevity. J. Immunol. **178:**7794–7804.
38. **Chang WL, Baumgarth N, Yu D, Barry PA.** 2004. Human cytomegalovirus-encoded interleukin-10 homolog inhibits maturation of dendritic cells and alters their functionality. J. Virol. **78:**8720–8731.
39. **Buffet PA, Safeukui I, Deplaine G, Brousse V, Prendki V, Thellier M, Turner GD, Mercereau-Puijalon O.** 2011. The pathogenesis of Plasmodium falciparum malaria in humans: insights from splenic physiology. Blood **117:**381–392.
40. **Del Portillo HA, Ferrer M, Brugat T, Martin-Jaular L, Langhorne J, Lacerda MV.** 2012. The role of the spleen in malaria. Cell Microbiol. **14:**343–355.
41. **Keller CC, Yamo O, Ouma C, Ong'echa JM, Ounah D, Hittner JB, Vulule JM, Perkins DJ.** 2006. Acquisition of hemozoin by monocytes down-regulates interleukin-12 p40 (IL-12p40) transcripts and circulating IL-12p70 through an IL-10-dependent mechanism: in vivo and in vitro findings in severe malarial anemia. Infect. Immun. **74:**5249–5260.
42. **Koehler JW, Bolton M, Rollins A, Snook K, deHaro E, Henson E, Rogers L, Martin LN, Krogstad DJ, James MA, Rice J, Davison B, Veazey RS, Prabhu R, Amedee AM, Garry RF, Cogswell FB.** 2009. Altered immune responses in rhesus macaques co-infected with SIV and Plasmodium cynomolgi: an animal model for coincident AIDS and relapsing malaria. PLoS One **4:**e7139. doi:10.1371/journal.pone.0007139.
43. **Smith TG, Ayi K, Serghides L, McAllister CD, Kain KC.** 2002. Innate immunity to malaria caused by Plasmodium falciparum. Clin. Investig. Med. **25:**262–272.
44. **Urban BC, Ferguson DJ, Pain A, Willcox N, Plebanski M, Austyn JM, Roberts DJ.** 1999. Plasmodium falciparum-infected erythrocytes modulate the maturation of dendritic cells. Nature **400:**73–77.
45. **Urban BC, Mwangi T, Ross A, Kinyanjui S, Mosobo M, Kai O, Lowe B, Marsh K, Roberts DJ.** 2001. Peripheral blood dendritic cells in children with acute Plasmodium falciparum malaria. Blood **98:**2859–2861.
46. **Urban BC, Roberts DJ.** 2002. Malaria, monocytes, macrophages and myeloid dendritic cells: sticking of infected erythrocytes switches off host cells. Curr. Opin. Immunol. **14:**458–465.
47. **Urban BC, Todryk S.** 2006. Malaria pigment paralyzes dendritic cells. J. Biol. **5:**4.
48. **Couper KN, Barnes T, Hafalla JC, Combes V, Ryffel B, Secher T, Grau GE, Riley EM, de Souza JB.** 2010. Parasite-derived plasma microparticles contribute significantly to malaria infection-induced inflammation through potent macrophage stimulation. PLoS Pathog. **6:**e1000744. doi: 10.1371/journal.ppat.1000744.
49. **Couper KN, Blount DG, Wilson MS, Hafalla JC, Belkaid Y, Kamanaka M, Flavell RA, de Souza JB, Riley EM.** 2008. IL-10 from CD4CD25Foxp3CD127 adaptive regulatory T cells modulates parasite clearance and pathology during malaria infection. PLoS Pathog. **4:**e1000004. doi:10.1371/journal.ppat.1000004.
50. **Skorokhod OA, Alessio M, Mordmuller B, Arese P, Schwarzer E.** 2004. Hemozoin (malarial pigment) inhibits differentiation and maturation of human monocyte-derived dendritic cells: a peroxisome proliferator-activated receptor-gamma-mediated effect. J. Immunol. **173:** 4066–4074.
51. **Wykes M, Keighley C, Pinzon-Charry A, Good MF.** 2007. Dendritic cell biology during malaria. Cell Microbiol. **9:**300–305.
52. **Wykes MN, Good MF.** 2008. What really happens to dendritic cells during malaria? Nat. Rev. Microbiol. **6:**864–870.
53. **Orengo JM, Wong KA, Ocana-Morgner C, Rodriguez A.** 2008. A Plasmodium yoelii soluble factor inhibits the phenotypic maturation of dendritic cells. Malar. J. **7:**254.
54. **Awandare GA, Ouma Y, Ouma C, Were T, Otieno R, Keller CC, Davenport GC, Hittner JB, Vulule J, Ferrell R, Ong'echa JM, Perkins DJ.** 2007. Role of monocyte-acquired hemozoin in suppression of macrophage migration inhibitory factor in children with severe malarial anemia. Infect. Immun. **75:**201–210.
55. **Coban C, Ishii KJ, Kawai T, Hemmi H, Sato S, Uematsu S, Yamamoto M, Takeuchi O, Itagaki S, Kumar N, Horii T, Akira S.** 2005. Toll-like receptor 9 mediates innate immune activation by the malaria pigment hemozoin. J. Exp. Med. **201:**19–25.
56. **Keller CC, Davenport GC, Dickman KR, Hittner JB, Kaplan SS, Weinberg JB, Kremsner PG, Perkins DJ.** 2006. Suppression of prostaglandin E2 by malaria parasite products and antipyretics promotes overproduction of tumor necrosis factor-alpha: association with the pathogenesis of childhood malarial anemia. J. Infect. Dis. **193:**1384–1393.
57. **Nti BK, Slingluff JL, Keller CC, Hittner JB, Ong'echa JM, Murphey-Corb M, Perkins DJ.** 2005. Stage-specific effects of Plasmodium falciparum-derived hemozoin on blood mononuclear cell TNF-alpha regulation and viral replication. AIDS **19:**1771–1780.
58. **Chang JJ, Lacas A, Lindsay RJ, Doyle EH, Axten KL, Pereyra F, Rosenberg ES, Walker BD, Allen TM, Altfeld M.** 2012. Differential regulation of toll-like receptor pathways in acute and chronic HIV-1 infection. AIDS **26:**533–541.
59. **Fischer-Smith T, Tedaldi EM, Rappaport J.** 2008. CD163/CD16 coexpression by circulating monocytes/macrophages in HIV: potential biomarkers for HIV infection and AIDS progression. AIDS Res. Hum. Retrovir. **24:**417–421.
60. **Granelli-Piperno A, Golebiowska A, Trumpfheller C, Siegal FP, Steinman RM.** 2004. HIV-1-infected monocyte-derived dendritic cells do not undergo maturation but can elicit IL-10 production and T cell regulation. Proc. Natl. Acad. Sci. U. S. A. **101:**7669–7674.
61. **Kim WK, Alvarez X, Fisher J, Bronfin B, Westmoreland S, McLaurin J, Williams K.** 2006. CD163 identifies perivascular macrophages in normal and viral encephalitic brains and potential precursors to perivascular macrophages in blood. Am. J. Pathol. **168:**822–834.
62. **Kim WK, Sun Y, Do H, Autissier P, Halpern EF, Piatak M, Jr, Lifson JD, Burdo TH, McGrath MS, Williams K.** 2010. Monocyte heterogeneity underlying phenotypic changes in monocytes according to SIV disease stage. J. Leukoc. Biol. **87:**557–567.
63. **Wu L, Kewal Ramani VN.** 2006. Dendritic-cell interactions with HIV: infection and viral dissemination. Nat. Rev. Immunol. **6:**859–868.
64. **Ocana-Morgner C, Wong KA, Rodriguez A.** 2008. Interactions between dendritic cells and CD4+ T cells during Plasmodium infection. Malar. J. **7:**88.
65. **May J, Lell B, Luty AJ, Meyer CG, Kremsner PG.** 2000. Plasma interleukin-10:tumor necrosis factor (TNF)-alpha ratio is associated with TNF promoter variants and predicts malarial complications. J. Infect. Dis. **182:** 1570–1573.
66. **Bentwich Z, Kalinkovich A, Weisman Z, Grossman Z.** 1998. Immune activation in the context of HIV infection. Clin. Exp. Immunol. **111:**1–2.
67. **Boasso A, Shearer GM.** 2008. Chronic innate immune activation as a cause of HIV-1 immunopathogenesis. Clin. Immunol. **126:**235–242.
68. **Duell BL, Tan CK, Carey AJ, Wu F, Cripps AW, Ulett GC.** 2012. Recent insights into microbial triggers of interleukin-10 production in the host and the impact on infectious disease pathogenesis. FEMS Immunol. Med. Microbiol. **64:**295–313.
69. **Mukherjee P, Devi YS, Chauhan VS.** 2008. Blood stage malaria antigens induce different activation-induced cell death programs in splenic CD4+T cells. Parasite Immunol. **30:**497–514.